

## Supporting Information

# Accelerated Click Reactions using Boronic Acids for Heterocyclic Synthesis in Microdroplets

Jyotirmoy Ghosh<sup>a</sup>, and R. Graham Cooks<sup>a,\*</sup>

<sup>a</sup>Department of Chemistry, Purdue University, 560 Oval Drive, West Lafayette, IN 47907, USA

\*To whom correspondence may be addressed. E-mail: [cooks@purdue.edu](mailto:cooks@purdue.edu)

## Table of Contents

<b>Experimental section</b>	S4
<b>Chemicals</b>	S4
<b>Drying procedure of acetonitrile solvent</b>	S4
<b>Nanoelectrospray ionization (nESI) source</b>	S4
<b>Spraying conditions and mass spectrometer parameters</b>	S4
<b>Suggested mechanism of superacid-catalyzed condensation</b>	S5
<b>Scale up for NMR spectroscopy</b>	S5

## Supplementary Figures

Figure S1	MS/MS spectra of product of reaction between butylamine and 2-formyl phenylboronic acid (2-FPBA) ( <i>m/z</i> 206)	S7
Figure S2	Comparison of the expected isotopic distribution and experimental mass spectra for iminoboronate product, <b>3</b>	S8
Figure S3	Comparison of the expected isotopic distribution and experimental mass spectra for reaction product, <b>5</b>	S9
Figure S4	MS/MS fragmentations pathway for boroxine product, <b>[4+H]<sup>+</sup></b>	S10
Figure S5	Comparison of the expected isotopic distribution and experimental mass spectra for boroxine product, <b>4</b>	S11
Figure S6	Comparison of <sup>11</sup> B-NMR spectra of standard 2-FPBA and boroxine product, <b>4</b>	S12
Figure S7	<sup>1</sup> H-NMR spectrum for boroxine product, <b>4</b>	S13
Figure S8	The addition effect of water for the reaction between butylamine and 2-FPBA	S14
Figure S9	Comparison of the expected isotopic distribution and experimental mass spectra for thiazolidine product, <b>9</b>	S15
Figure S10	MS/MS fragmentations pathway for isomeric diazaborine	S16

	products, <b>12</b> and <b>14</b>	
Figure S11	Comparison of the expected isotopic distribution and experimental mass spectra for isomeric diazaborine products, <b>12</b> and <b>14</b>	S17
Figure S12	<sup>11</sup> B-NMR spectrum for diazaborine products, <b>12</b> and <b>14</b>	S18
Figure S13	Comparison of the expected isotopic distribution and experimental mass spectra for late-stage functionalization (LSF) product of the antihistamine drug, <b>16</b>	S19
Figure S14	MS/MS spectra for LSF product of the antihistamine drug, <b>17</b>	S20
Figure S15	Comparison of the expected isotopic distribution and experimental mass spectra for LSF product of the antihistamine drug, <b>17</b>	S21
Figure S16	MS/MS spectra for LSF product of the antihistamine drug, <b>18</b>	S22
Figure S17	Comparison of the expected isotopic distribution and experimental mass spectra for LSF product of the antihistamine drug, <b>18</b>	S23
Figure S18	Mass spectrum of LSF products of benzhydrylpiperazine (antihistamine precursor)	S24
Figure S19	Mass spectrum of LSF products of diphenyl-4-piperidinemethanol (antihistamine precursor)	S25
Figure S20	Mass spectrum of LSF products of 2-((4-chlorophenyl)(piperidin-4-yloxy)methyl)pyridine (antihistamine precursor)	S26
Figure S21	Mass spectrum of LSF products of 4-(benzhydryloxy)piperidine (antihistamine precursor)	S27
Figure S22	Mass spectrum of LSF products of Desloratadine (antihistamine precursor)	S28

## **1. Experimental section**

### **1.1. Chemicals**

2-Formyl phenylboronic acid (2-FPBA, **1**) was purchased from Combi-Blocks, Inc. (San Diego, CA) and all the amines such as butylamine **2**, cysteamine **6**, and phenylhydrazine **10** were purchased from Sigma Aldrich (St. Louis, MO). All antihistamine precursors used in this study were sourced from Sigma Aldrich, Fisher Scientific, and Combi-Blocks, Inc.

### **1.2. Drying procedure of acetonitrile solvent**

Acetonitrile (ACN) solvent was dried, where noted, by stirring over CaH<sub>2</sub>, the drying agent for 24-72 hours, and then the solvent was distilled off the drying agent. After distillation, the solvent was stored over activated 4Å molecular sieves and kept in an air-sealed container. Note that prior to use, the molecular sieves were activated by heating under vacuum for 24 hours.

### **1.3. Nanoelectrospray ionization (nESI) source**

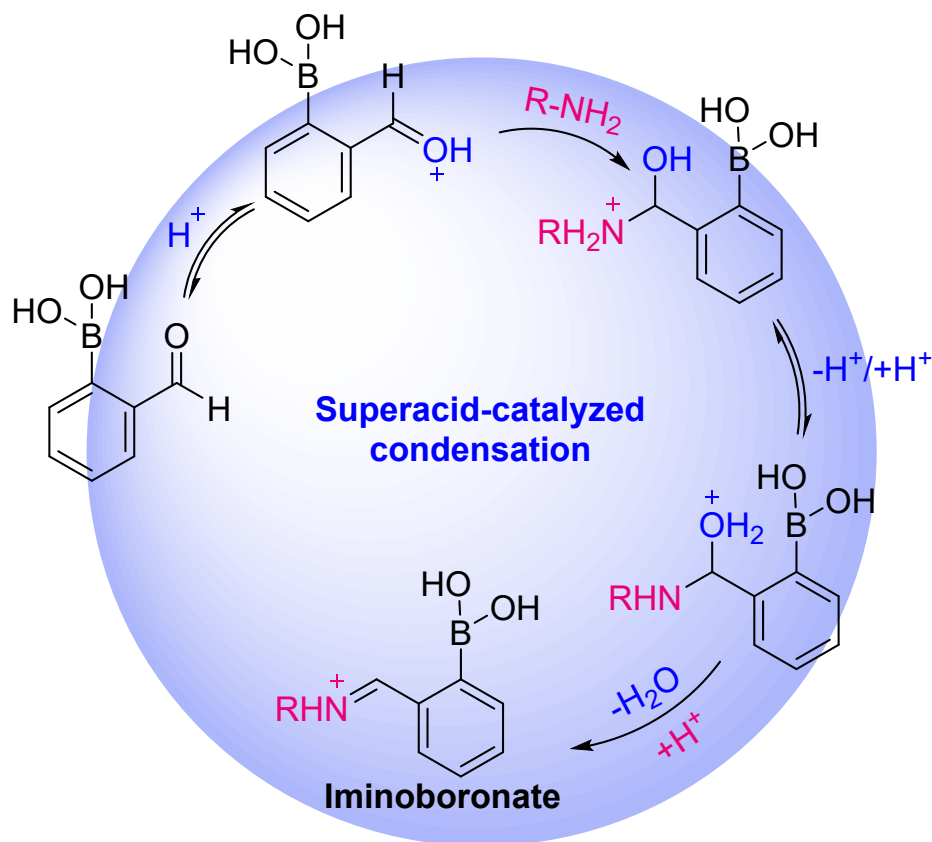
Borosilicate glass capillaries with dimensions of 1.5 mm O.D., 0.86 mm I.D., and 10 cm in length were acquired from Sutter Instruments (Novato, CA), which were used for nanoelectrospray ionization mass spectrometry (nESI-MS) analysis. Further, a micropipette puller (Model: P-97, Sutter Instruments, Novato, CA) was used to create nESI emitters with a 5 µm internal diameter of the tip. These emitters were filled with the reaction mixture solution and a stainless-steel electrode was inserted into the solution to apply high voltage. The reaction mixture was electrosprayed applying a positive DC potential of 1.5 kV to the nESI electrode and a 10 mm spray distance between the sprayer tip and MS inlet was maintained.

### **1.4. Spraying conditions and mass spectrometer parameters**

The reaction was performed by mixing equal volumes (25 µL) of amine and 2-formyl phenylboronic acid each 10 mM to give a final reaction mixture (5 mM, 50 µL). The reaction was performed in reagent grade ACN solvent without additional drying except where indicated. The mass spectra were recorded using a Thermo Fisher LTQ mass spectrometer (Thermo Scientific Inc., San Jose, CA). Ion source parameters for the MS analysis were a max injection time of 200 ms; capillary temperature of 150 °C; capillary voltage of 15 V; and tube lens of 65 V. Tandem mass spectrometry (MS/MS) was used for the structural characterization of ions of selected *m/z*

value. Please note that recorded experimental mass spectra are of unit resolution, while comparing with the isotopic distribution.

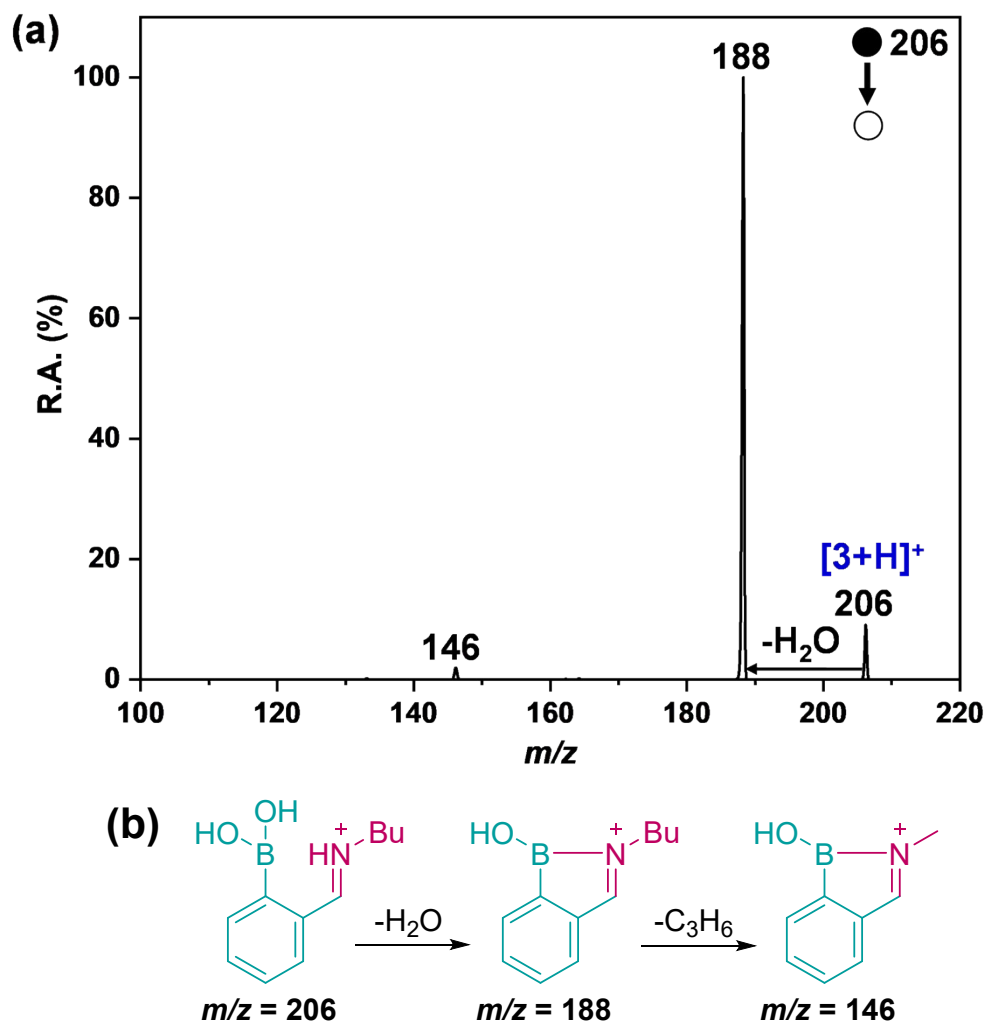
### 1.5. Suggested mechanism of superacid-catalyzed condensation



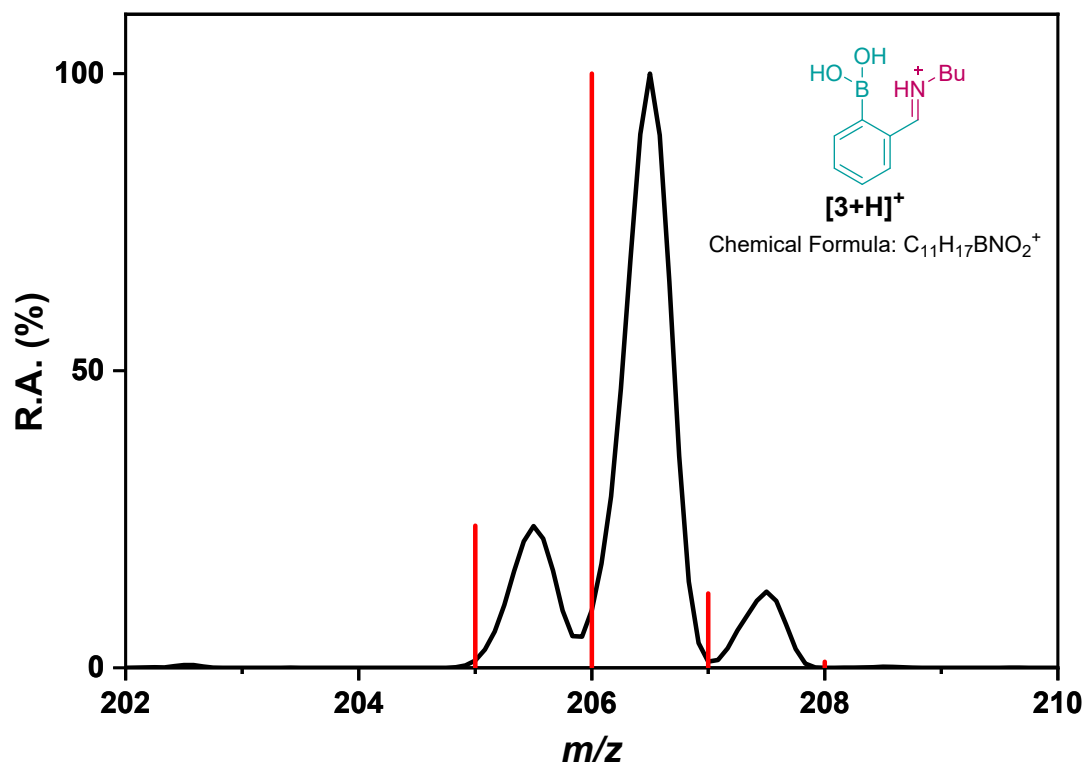
### 1.6. Scale up for NMR spectroscopy

Unless otherwise noted, the chemical reactions in microdroplets were scaled up by collecting the sprayed products for characterization by NMR spectroscopy. Before spraying, a 5 mL reaction mixture was placed in a glass syringe connected to a syringe pump (Hamilton, MA). The final concentration of the reaction mixture for all the reactions was 25 mM. The reaction mixtures were electrosprayed using a home-built electrosonic spray ionization (ESSI) source at a constant flow rate of 25  $\mu$ L/min while applying a positive DC potential of 1.5 kV. The nebulization gas (N<sub>2</sub>) pressure was 40 psi. Electrosprayed microdroplets were collected by inserting the sprayer tip in a glass test tube closed with a rubber septum to minimize the loss of products upon collection. Two open-ended hypodermic needles were inserted through the septum, one of which acted as an outlet

for nebulization gas. Unless otherwise noted, the distance from the sprayer to the glassware surface was 2 cm. The collection experiment was done for 60 minutes at room temperature to obtain 0.5 - 3.25 mg amounts of product, which was dissolved in  $\text{CDCl}_3$  for NMR analysis.

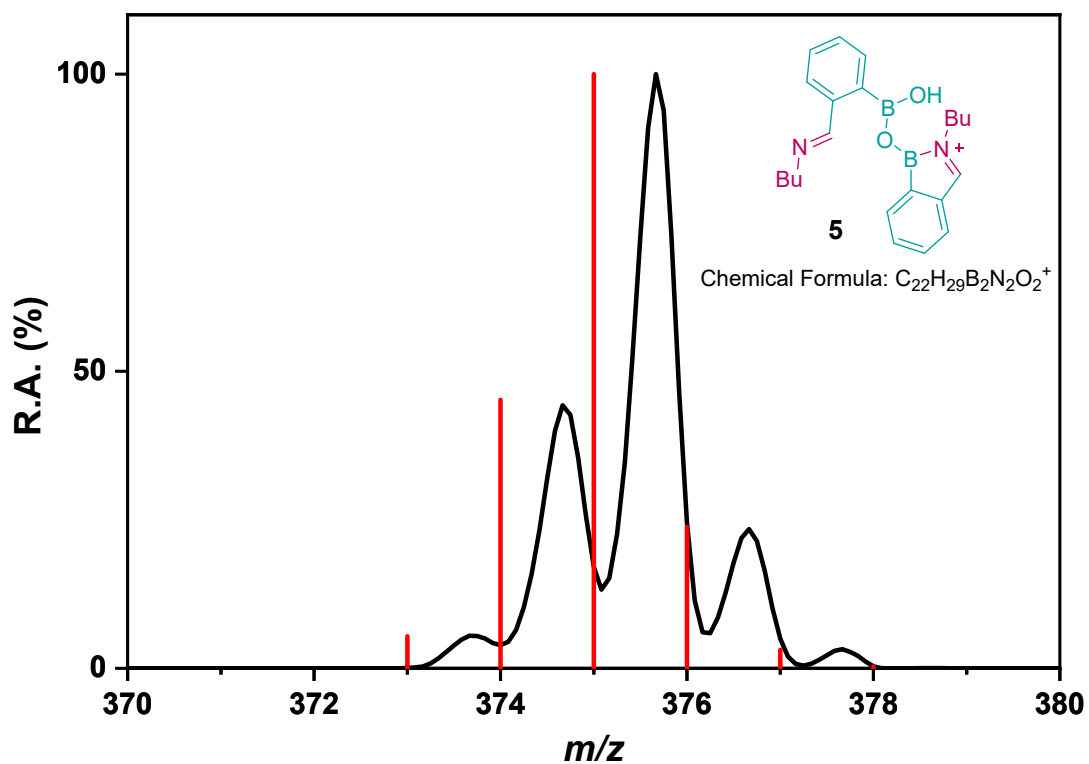


**Figure S1.** (a) Positive mode product ion MS/MS spectrum of mass-selected iminoboronate product, **3**. (b) Corresponding MS/MS fragmentations are rationalized in the scheme and structures of the fragment ions are suggested.

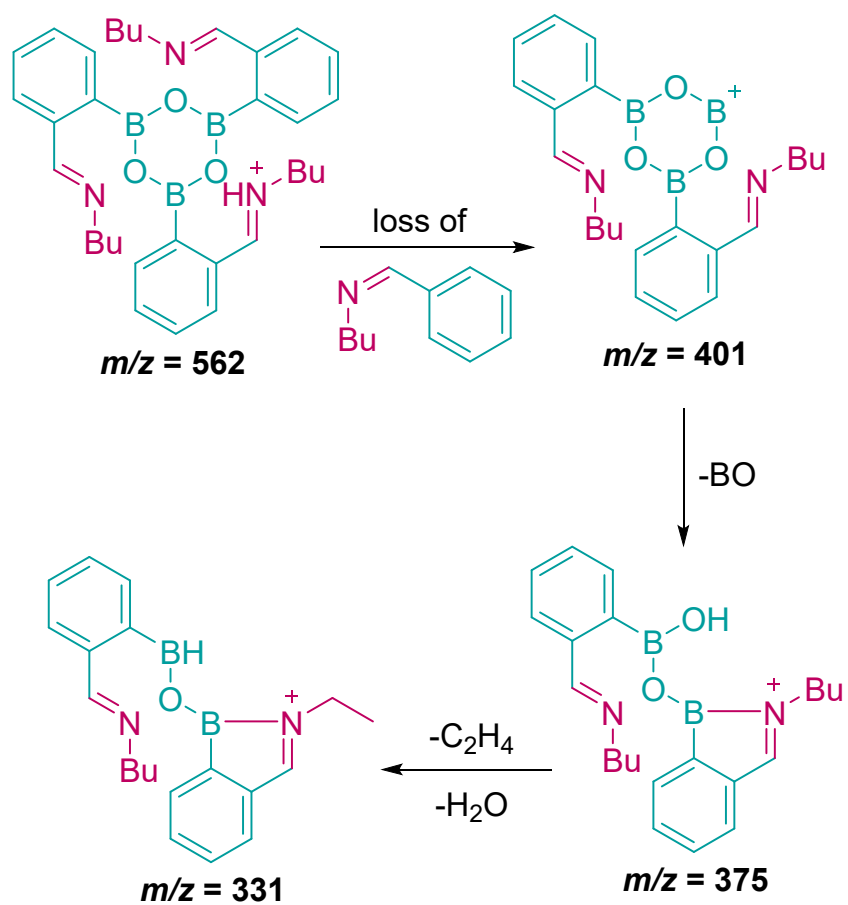


**Figure S2.** Comparison of the expected isotopic distribution and experimental mass spectra for iminoboronate product, **3**. The suggested structure of the product ion is shown in the inset.

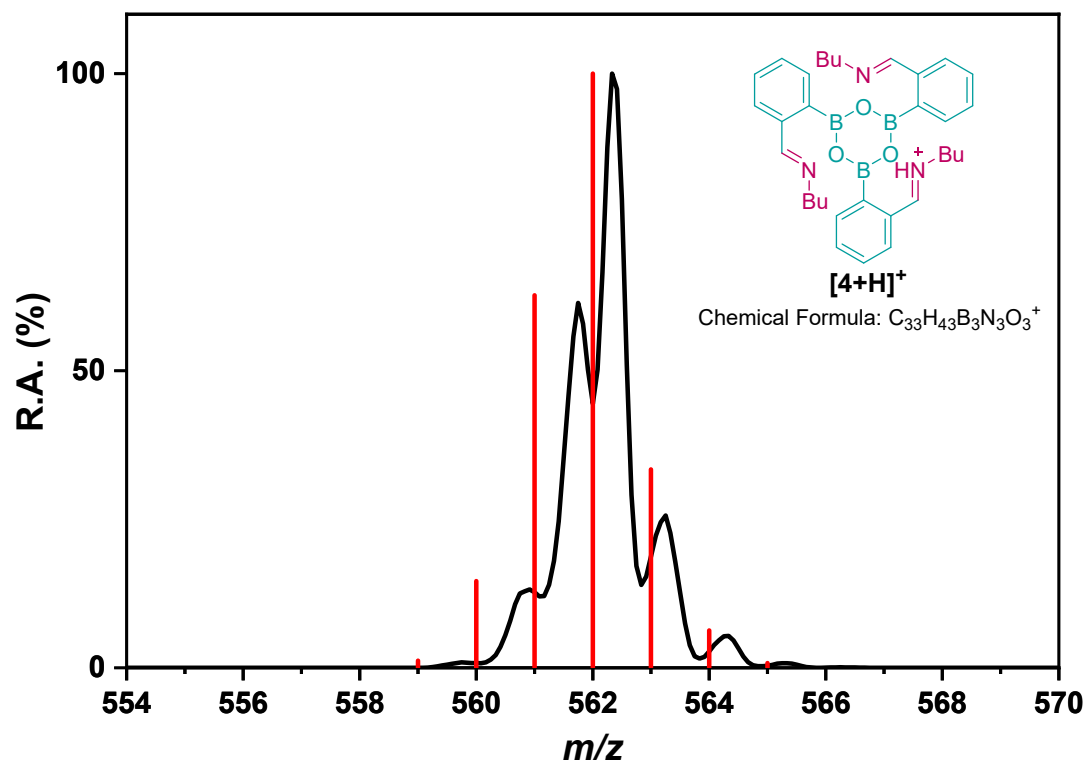




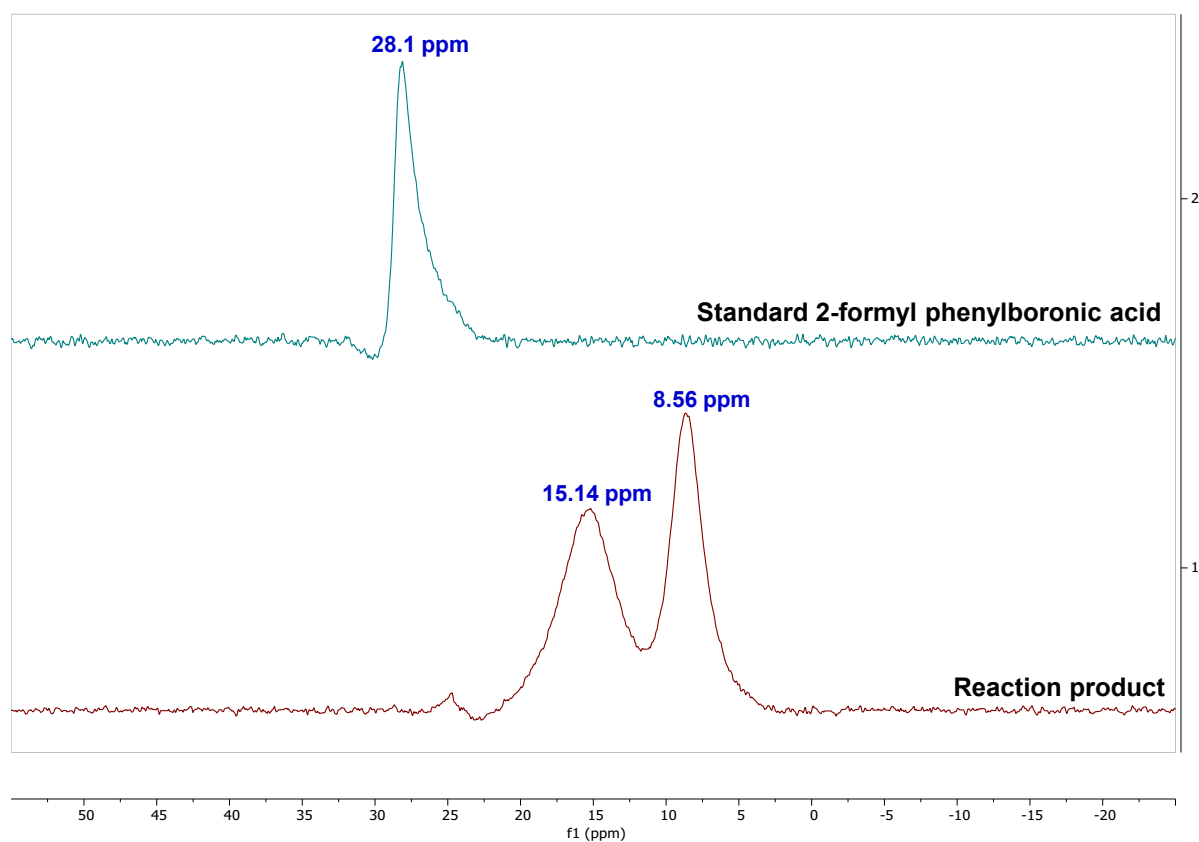
**Figure S3.** Comparison of the expected isotopic distribution and experimental mass spectra for dehydration dimer product, **5**. The suggested structure of the product ion is shown in the inset.



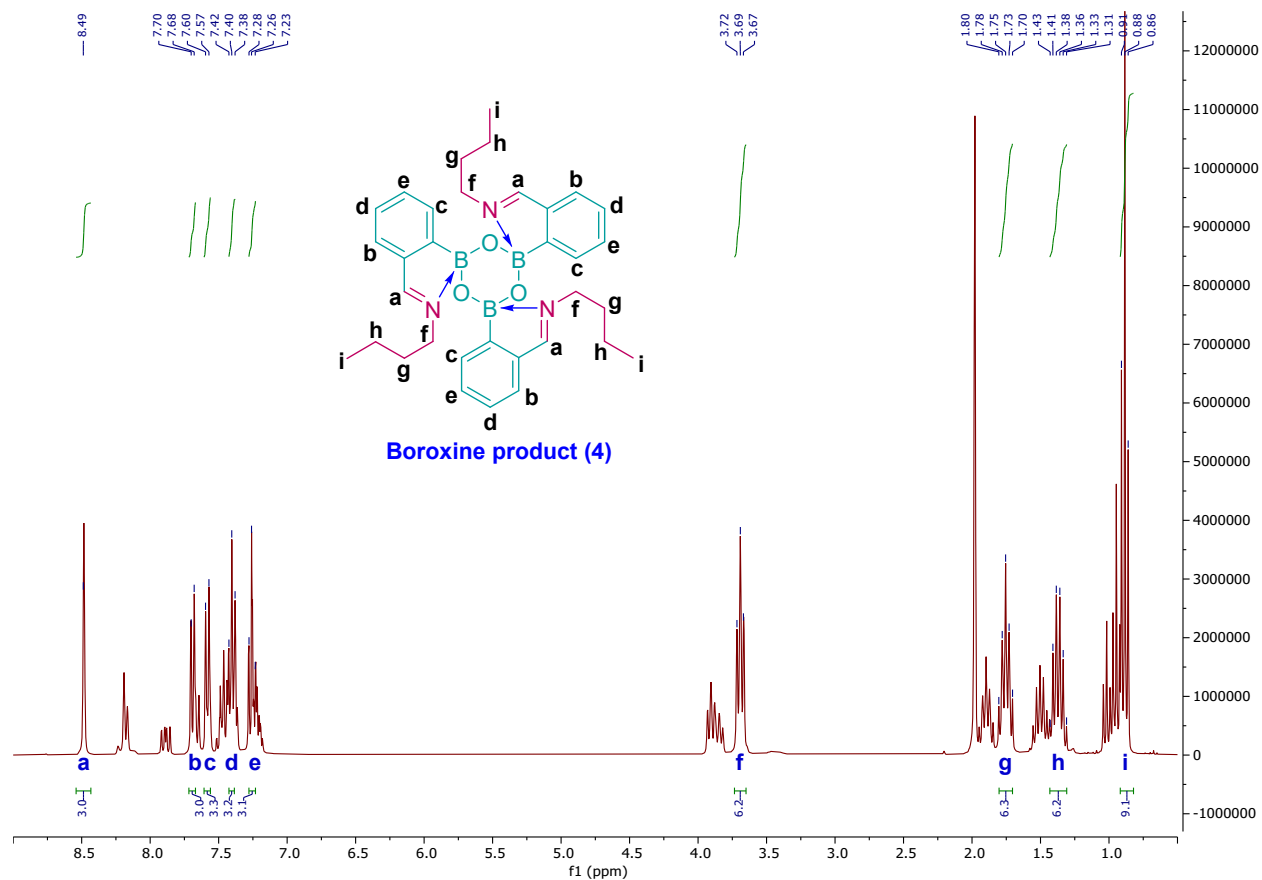
**Figure S4.** MS/MS fragmentations pathway for boroxine product,  $[4+H]^+$  product is rationalized.



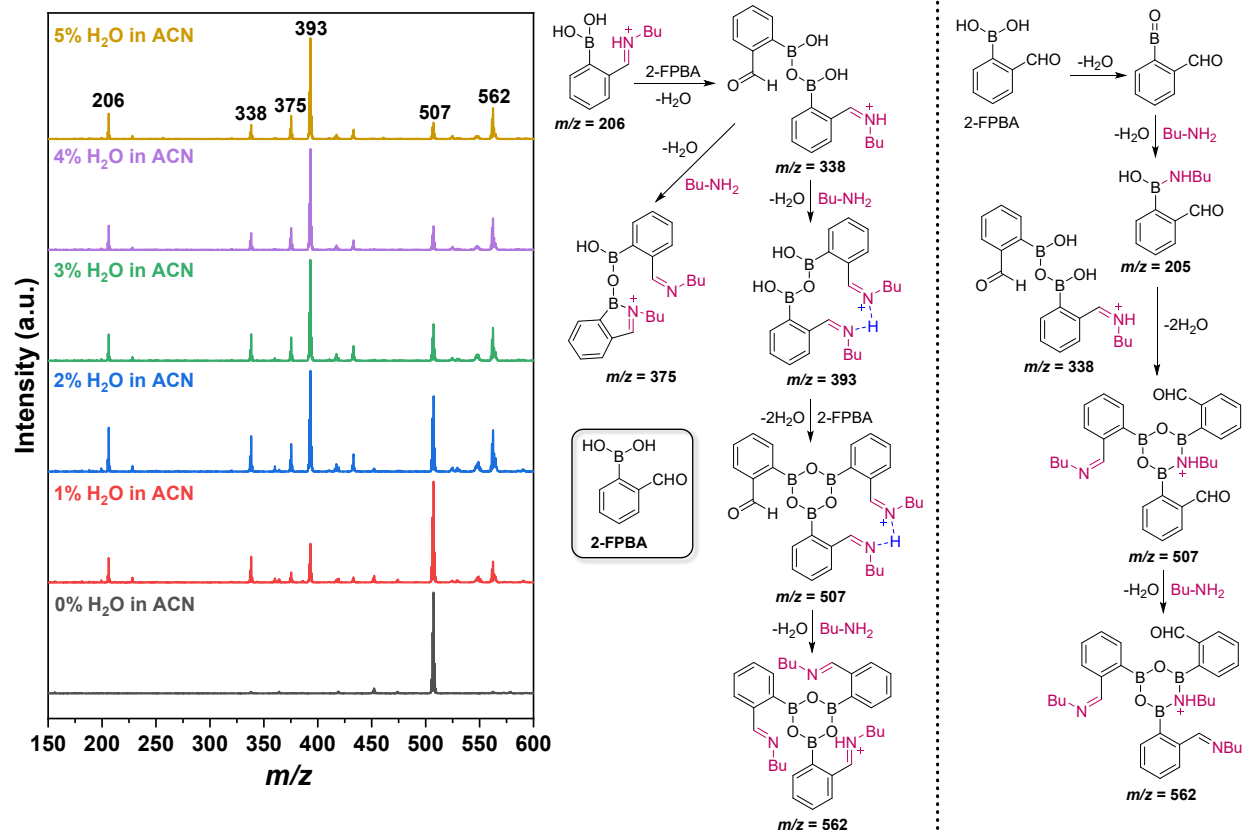
**Figure S5.** Comparison of the expected isotopic distribution and experimental mass spectra for the boroxine product, **4**. The suggested structure of the product ion is shown in the inset.



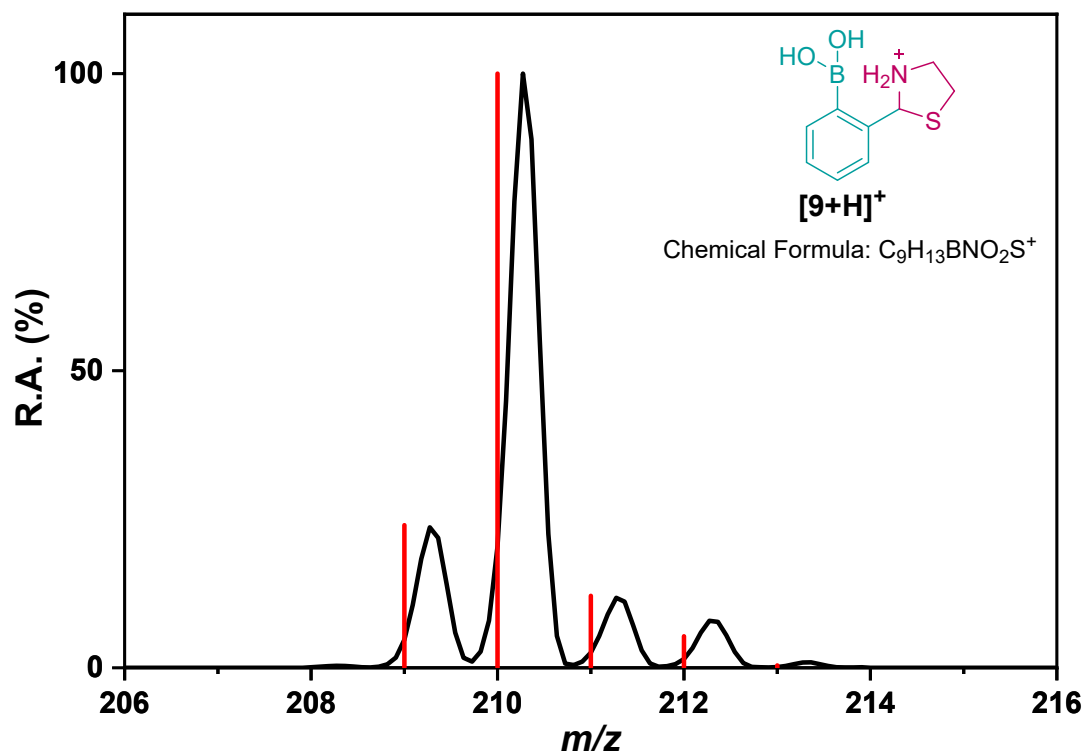
**Figure S6.** Comparison of  $^{11}\text{B}$ -NMR spectra (300 MHz,  $\text{CDCl}_3$ ) of standard 2-formyl phenylboronic acid and the reaction product obtained by electrospraying butylamine and 2-formyl phenylboronic acid microdroplets. The NMR peak at 15.14 ppm corresponds to the boroxine, **4**, much shifted from the starting reagent 2-formyl phenylboronic acid (28.1 ppm). The other peak at 8.56 ppm may arise from other products shown in Figure 1.



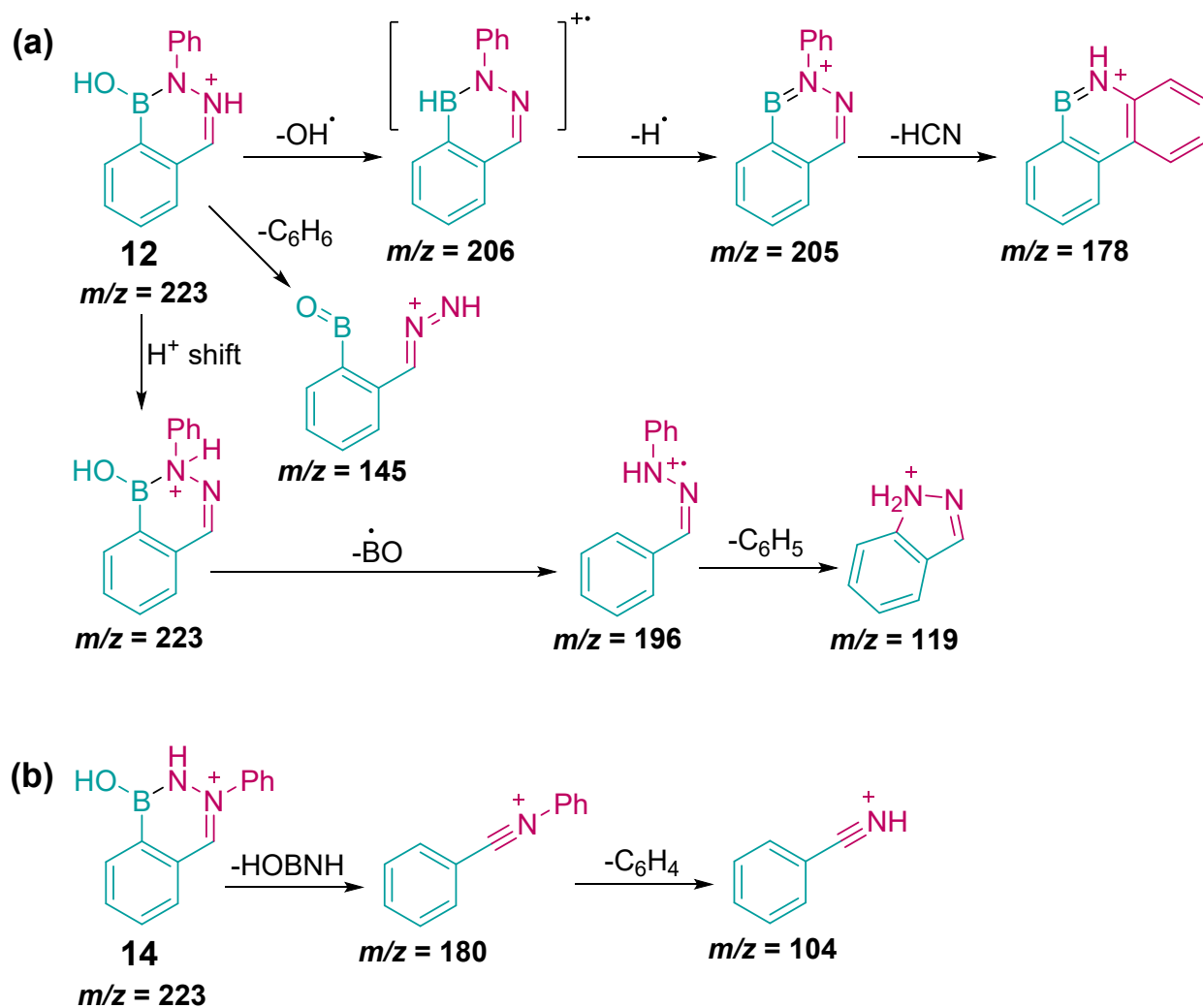
**Figure S7.** <sup>1</sup>H-NMR spectrum of the products of reaction between butylamine and 2-formyl phenylboronic acid in microdroplets recorded without purification. The spectrum shows the presence of boroxine, **4** as the major product along with the other products as shown in Figure 1. The NMR peaks for all the equivalent protons (H<sub>a</sub>-H<sub>i</sub>) in the boroxine structure are assigned as shown in the inset. <sup>1</sup>H-NMR (300 MHz, CDCl<sub>3</sub>) δ 8.49 (s, 3H), 7.69 (d, J = 6.6 Hz, 3H), 7.58 (d, J = 7.4 Hz, 3H), 7.40 (t, 3H), 7.28 – 7.23 (m, 3H), 3.69 (t, J = 7.1 Hz, 6H), 1.75 (t, J = 7.5 Hz, 6H), 1.36 (dt, J = 14.7, 7.4 Hz, 6H), 0.88 (t, J = 7.3 Hz, 9H).



**Figure S8.** Positive mode nESI mass spectra of products of the reaction between butylamine and 2-FPBA in different ratios of H<sub>2</sub>O:ACN microdroplets. Suggested chemical structures for observed ionic forms of the reaction products are illustrated on the right side. Here, 0% H<sub>2</sub>O in ACN refers to the specially dried ACN solvent (see Experimental section 1.2 in SI).

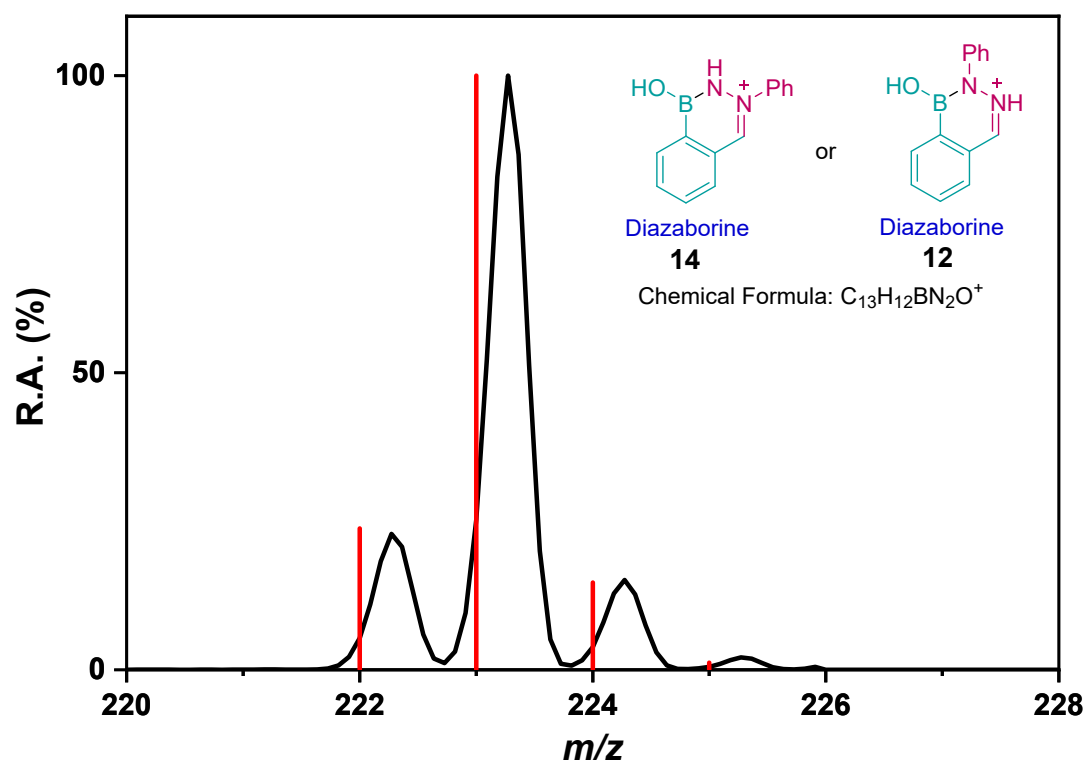


**Figure S9.** Comparison of the expected isotopic distribution and experimental mass spectra for thiazolidine product,  $[9+H]^+$ . The structure of the product ion is shown in the inset.

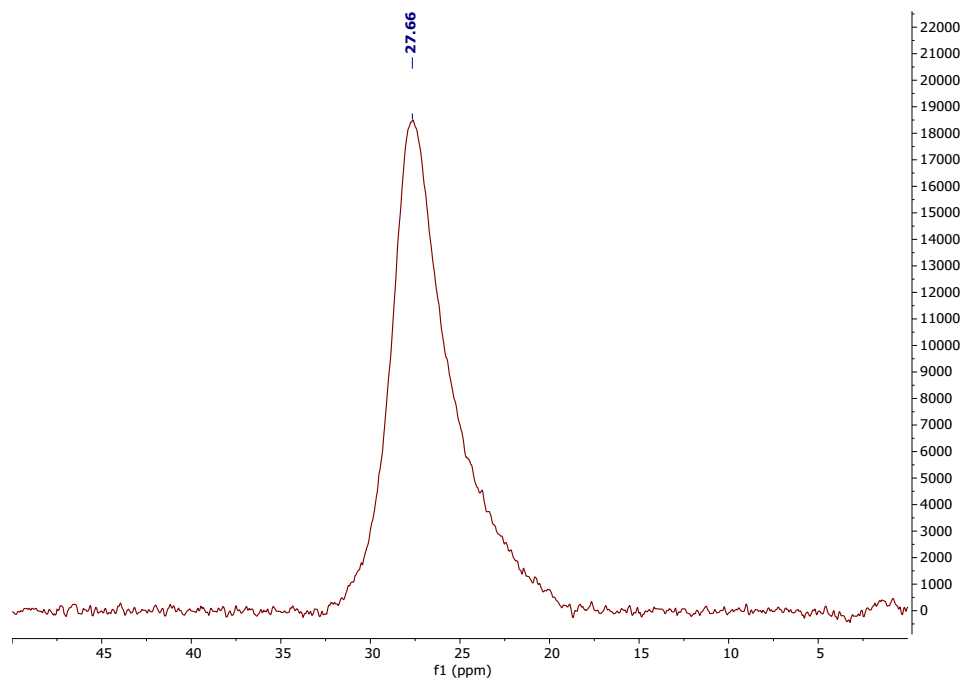


**Figure S10.** Rationalization of MS/MS fragmentation pathways for the isomeric diazaborine products (a) compound 12 and (b) compound 14.

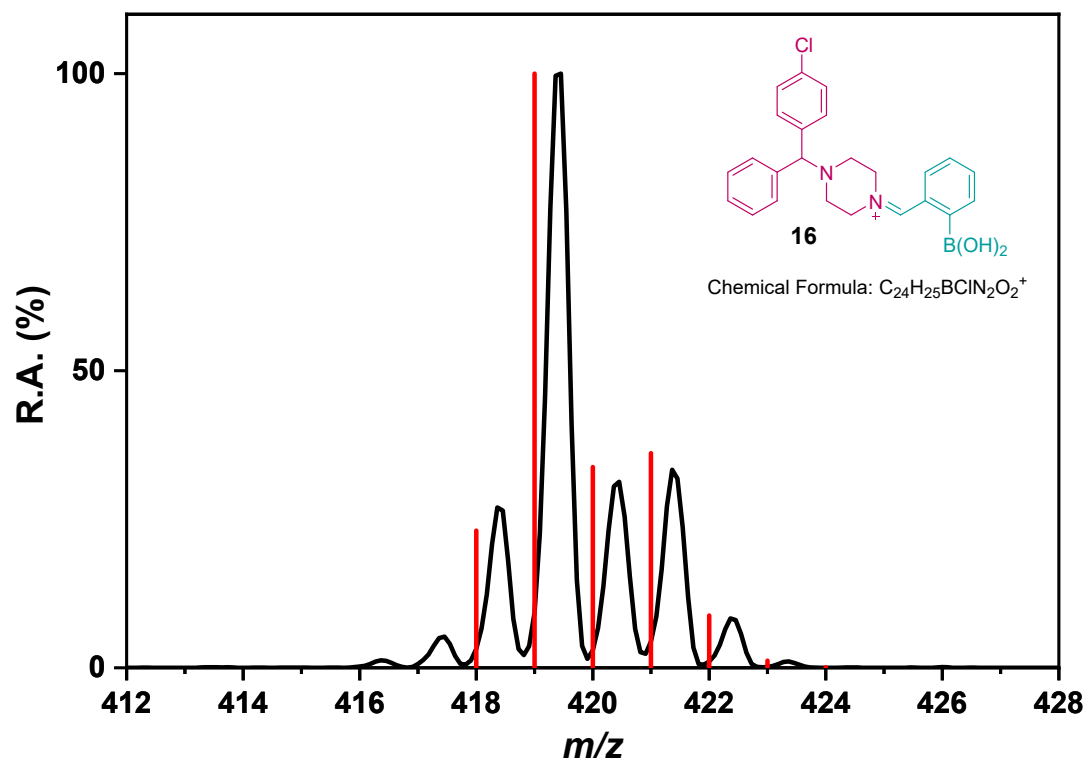




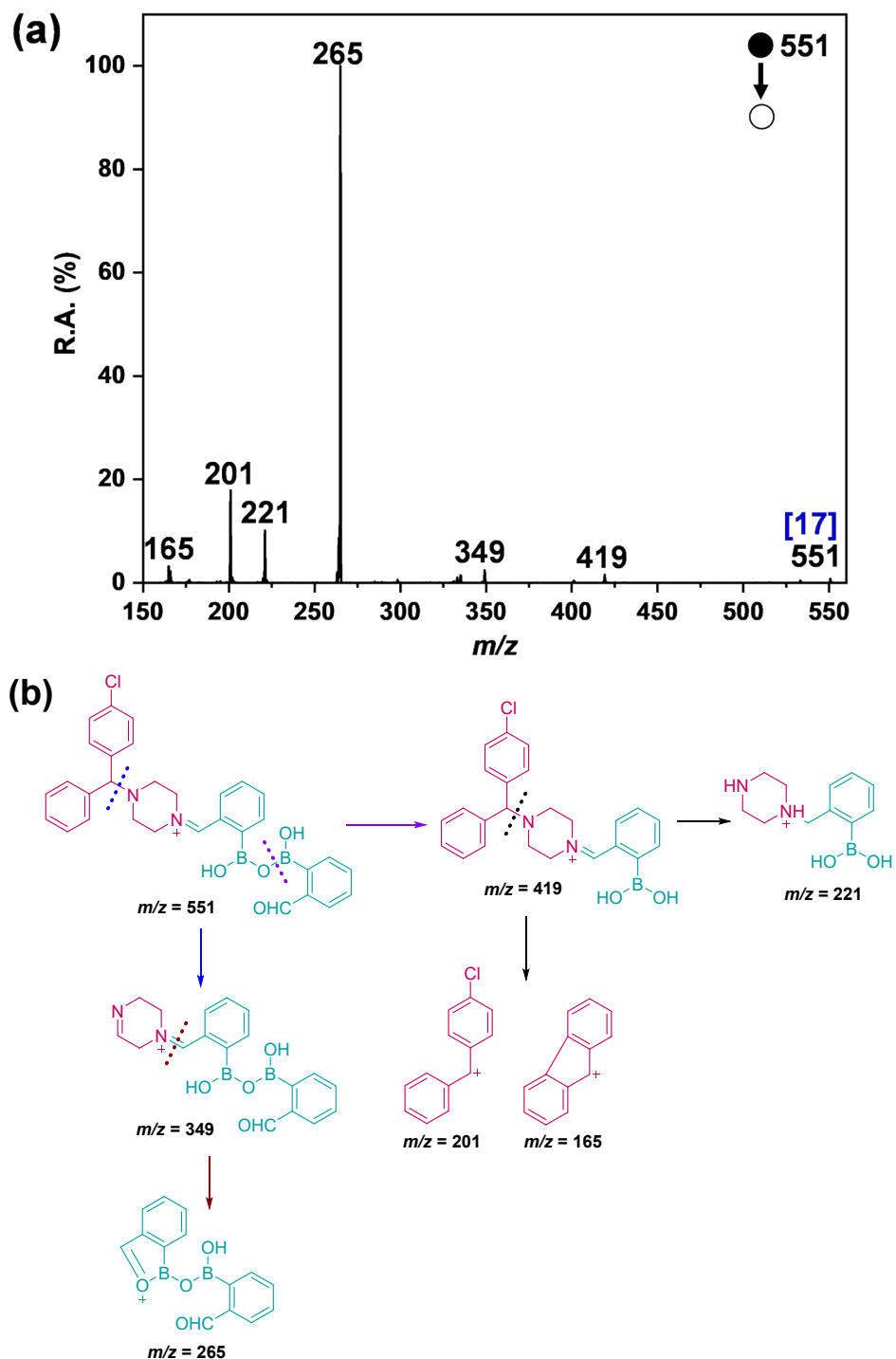
**Figure S11.** Comparison of the expected isotopic distribution and experimental mass spectra for isomeric diazaborine products, **12** and **14**. The structures of the product ions are shown in the inset.



**Figure S12.**  $^{11}\text{B}$ -NMR spectrum of the products of reaction between phenylhydrazine and 2-formyl phenylboronic acid in microdroplets, taken without purification. The spectrum shows the presence of diazaborine product, **12** or **14**.  $^{11}\text{B}$  NMR (300 MHz,  $\text{CDCl}_3$ )  $\delta$  27.66 (s).



**Figure S13.** Comparison of the expected isotopic distribution and experimental mass spectra for the late-stage functionalization (LSF) product of the antihistamine drug, **16**. The suggested structure of the product ion is shown in the inset.



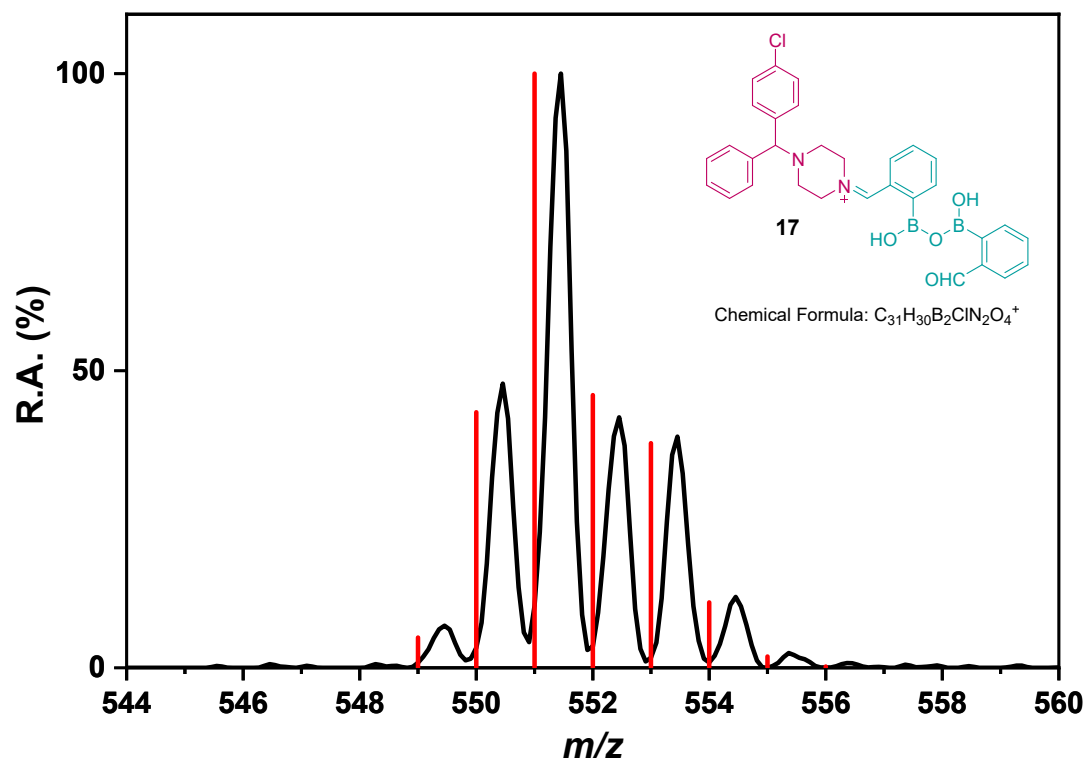


**Figure S15.** Comparison of the expected isotopic distribution and experimental mass spectra for the LSF product of antihistamine drug, **17**. The suggested structure of the ion is shown in the inset.

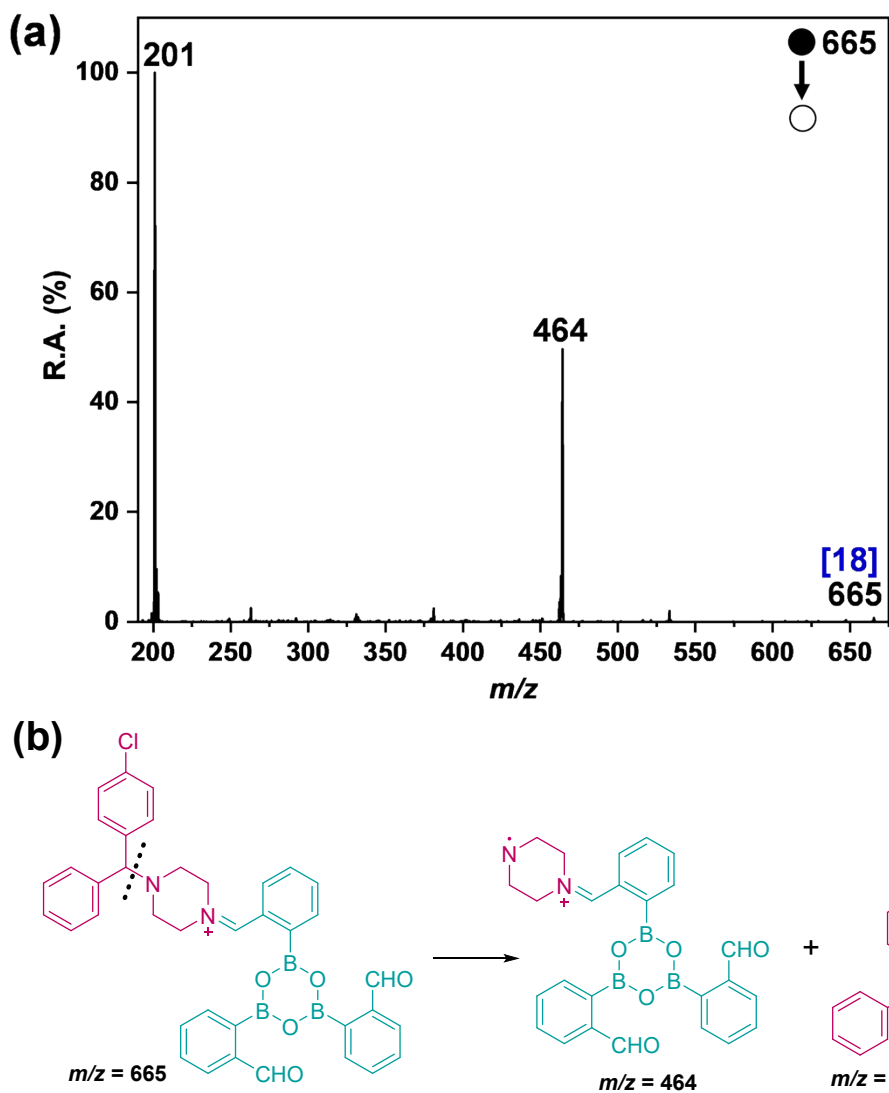


**Figure S16.** (a) Positive mode product ion MS/MS spectrum of mass-selected antihistamine LSF product, **18**. (b) Corresponding MS/MS fragmentations are rationalized in the scheme and structures of the fragment ions are suggested.

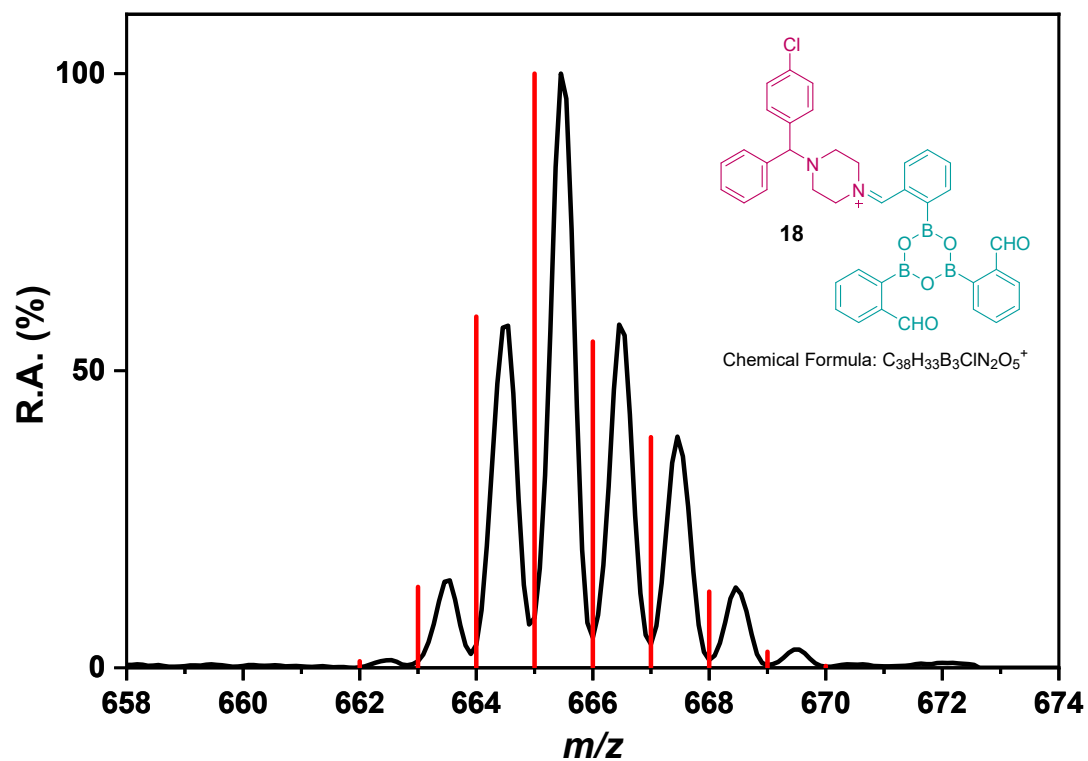


**Figure S17.** Comparison of the expected isotopic distribution and experimental mass spectra for the LSF product of antihistamine drug, **18**. The suggested structure of the product ion is shown in the inset.

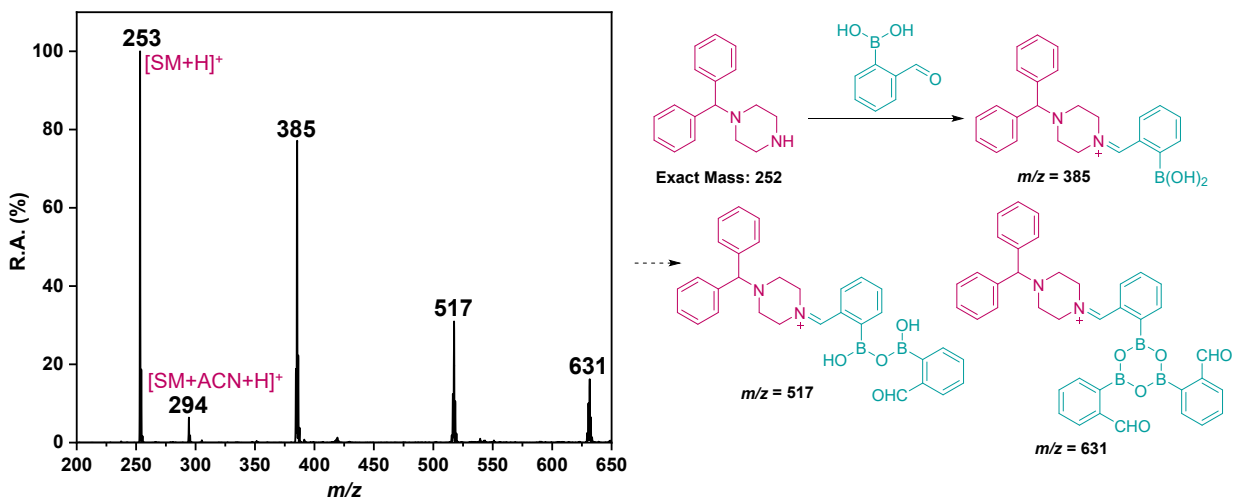


**Figure S18.** Positive mode mass spectrum of the reaction between benzhydrylpiperazine (antihistamine drug), and 2-formyl phenylboronic acid in ACN microdroplets. Here, the protonated form of the drug (starting material) and the cluster of starting material and ACN are represented as  $[SM+H]^+$  and  $[SM+ACN+H]^+$ , respectively. The suggested structures of the product ions are shown on the right.



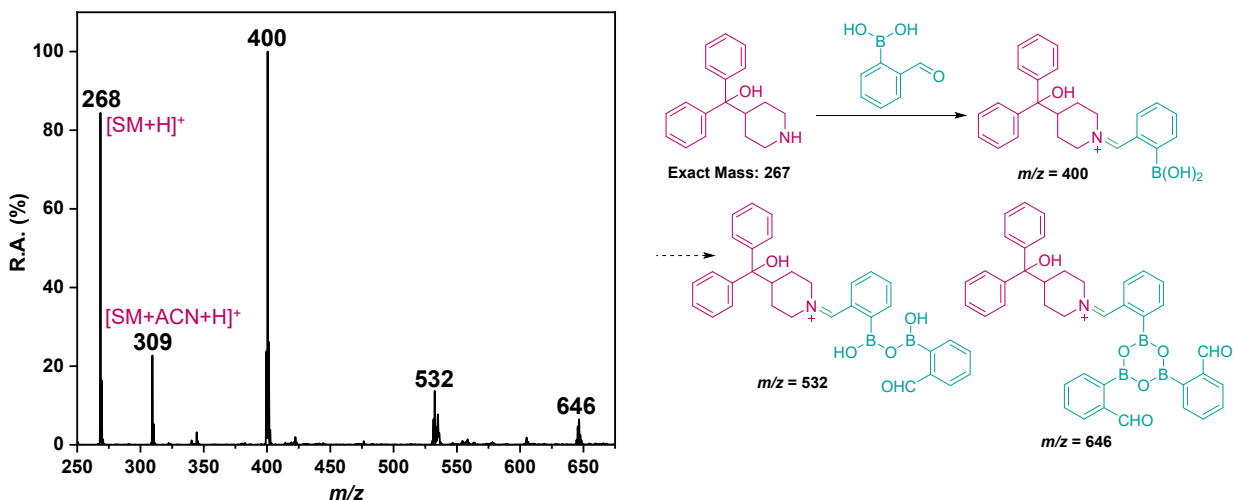


**Figure S19.** Positive mode mass spectrum of the product of reaction between diphenyl-4-piperidinemethanol (antihistamine drug precursor) and 2-formyl phenylboronic acid in ACN microdroplets. Here, the protonated form of the drug (starting material) and the cluster of starting material and ACN are represented as [SM+H]<sup>+</sup> and [SM+ACN+H]<sup>+</sup>, respectively. The suggested structures of the product ions are shown on the right.

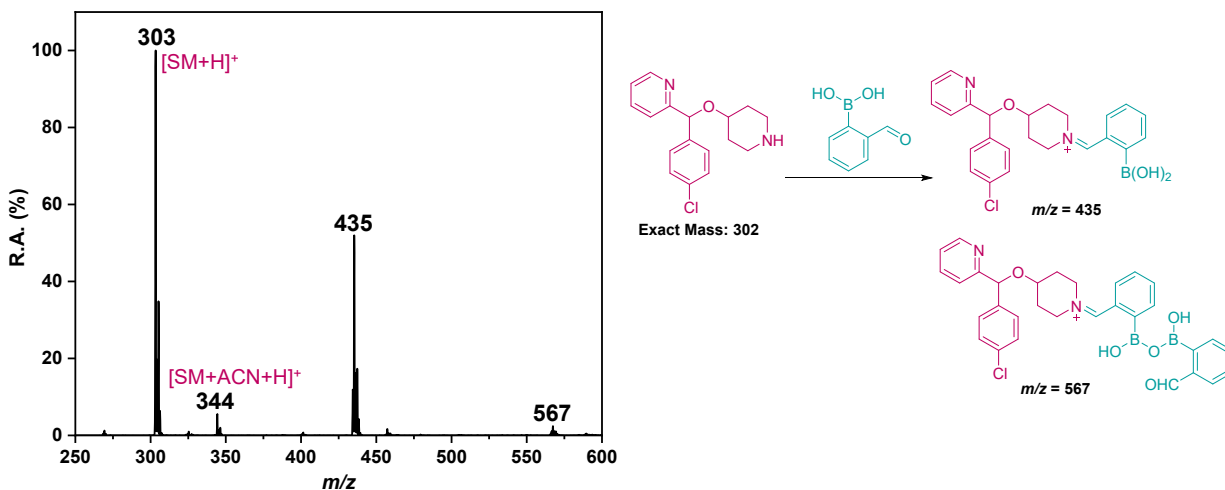


**Figure S20.** Positive mode mass spectrum of the products of reaction between 2-((4-chlorophenyl)(piperidin-4-yloxy)methyl)pyridine (antihistamine drug precursor) and 2-formyl phenylboronic acid in ACN microdroplets. Here, the protonated form of the drug (starting material) and the cluster of strating material and ACN are represented as  $[SM+H]^+$  and  $[SM+ACN+H]^+$ , respectively. The suggested structures of the product ions are shown on the right.

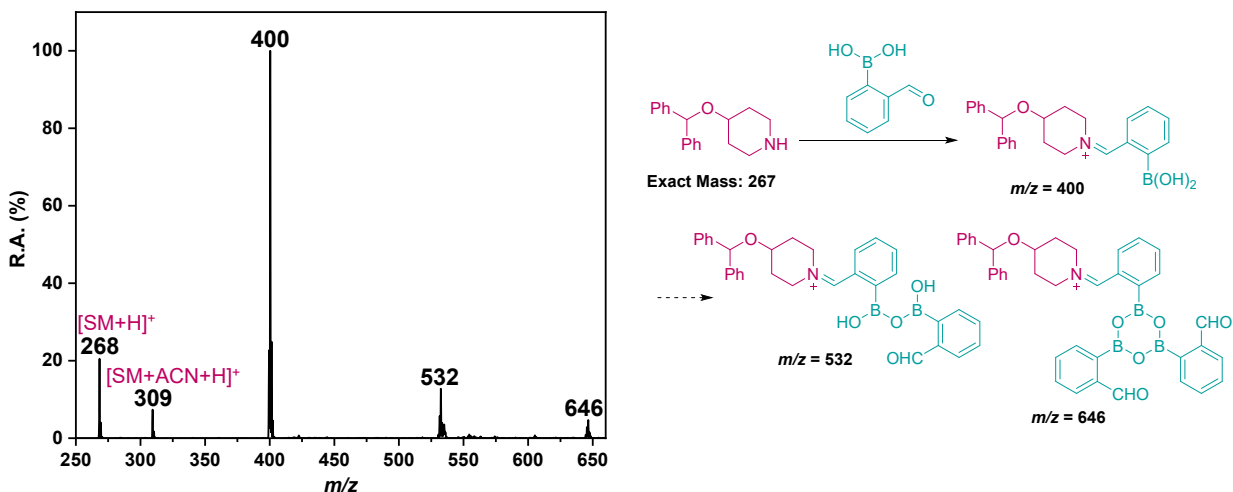


**Figure S21.** Positive mode mass spectrum of the products of reaction between 4-(benzhydryloxy)piperidine (antihistamine drug precursor) and 2-formyl phenylboronic acid in ACN microdroplets. Here, the protonated form of the drug (starting material) and the cluster of starting material and ACN are represented as  $[SM+H]^+$  and  $[SM+ACN+H]^+$ , respectively. The suggested structures of the product ions are shown on the right.

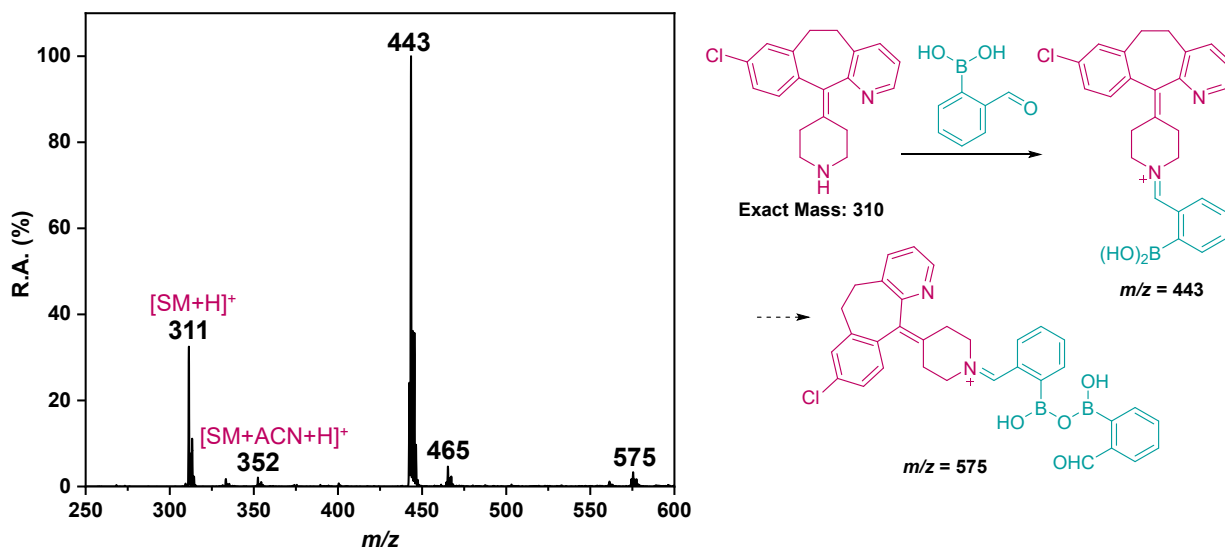


**Figure S22.** Positive mode mass spectrum of the products of reaction between Desloratidine (antihistamine drug precursor) and 2-formyl phenylboronic acid in ACN microdroplets. Here, the protonated form of the drug (starting material) and the cluster of strating material and ACN are represented as  $[SM+H]^+$  and  $[SM+ACN+H]^+$ , respectively. The suggested structures of the product ions are shown on the right and the peak at  $m/z$  465 corresponds to the  $Na^+$  adduct of the most abundant product.